Coastal Boundary-Layer Characteristic During Night Time Using a Long-Term Acoustic Remote Sensing Data

Damyan Barantiev and Ekaterina Batchvarova

Abstract The study of the Planetary Boundary Layer vertical structure in coastal areas is of particular importance due to the fact that a large number of urban areas and their industrial activities are located on the shores of the seas, oceans or large lakes. Based on long-term (August 2008–October 2016) sodar measurements at a Bulgarian Black Sea coastal site, the mean characteristics of the two main types of nocturnal air flows (marine and land air masses) are obtained. Typical parameters for the investigated region, such as the heights of the marine, the internal and planetary boundary layers, as well as wind and turbulence vertical structure details are revealed exploring this high spatial (10 m) and temporal (10 min) resolution data. The observation site is near the town of Ahtopol in Southeast Bulgaria. The analyses are based on averaging of the measured profiles of 12 output sodar parameters and calculated Buoyancy Production mean profiles. The seasonal variability of all characteristics is explored. The nocturnal land air masses are found to be with neutral and slightly stable stratification, Planetary Boundary-Layer height of 410–430 m and corresponding Surface-Layer height of 50–80 m. The nocturnal marine air masses are found to be with neutral and slightly unstable stratification, Internal Boundary-Layer height of about 40–50 m and a nocturnal marine Planetary Boundary-Layer height of about 300 m. The study contributes to disclosure and understanding the coastal nocturnal wind and turbulence regime in a region with modest observation networks. The obtained results can be also used for evaluation of the various theoretical, mesoscale and air quality models performance.

Keywords Sodar · Remote sensing data · Wind and turbulent profiles · Black sea · Coastal area · PBL · Climatological studies

D. Barantiev (✉) · E. Batchvarova
Climate, Atmosphere and Water Research Institute—Bulgarian Academy of Sciences, CAWRI—BAS, 66, Tsarigradsko Shose blvd, 1784 Sofia, Bulgaria
e-mail: dbarantiev@cawri.bas.bg

N. Dobrinkova and G. Gadzhev (eds.), *Environmental Protection and Disaster Risks*, Studies in Systems, Decision and Control 361,
https://doi.org/10.1007/978-3-030-70190-1_4

1 Introduction

The significant technological development of ground-based instruments for remote measurements of atmospheric characteristics during the last years places them among the reliable and indispensable instruments in a number of innovative scientific methods for the study of the main meteorological parameters and turbulence in the Planetary Boundary Layer (PBL) [1–6]. Substantial interest in studying the coastal PBL is the complexity of the processes observed in air masses transformation due to the sharp change in the physical characteristics of the surface. The challenges in describing coastal processes are related to Internal Boundary Layer (IBL) formation and its evolution as a sublayer of PBL when marine airflow comes over land and define its spatial scales with a height dependent on the distance from the shore [7, 8]. Due to the formation of such sublayers with different thermodynamical states and the presence of local circulation in the coastal zones (breeze), the atmosphere is complexly stratified, resulting in intricate processes of air pollution dispersion compared to regions with homogeneous surface [9].

A number of scientific experiments with doppler lidars, sodars, high meteorological masts, surface and aerological measurements aim to provide data to evaluate the mesometeorological models performance in coastal areas and to ensure further development of parameterizations.

Wilczak et al. [10] present the results of a complex experiment to study varying scales of airflows in California's coastal zone, with a center in Santa Barbara. The experiment was conducted on September 20, 1985. Doppler wind lidars, sodars, multiple stations with surface observations, and radio sounding were used. Part of the sodars measurements were also carried out at the platforms in the ocean. These data were used to verify the accuracy of mesometeorological models' simulations.

An IBL study in a complex coastal area was based on airborne lidar measurements, mesometeorological modeling with CSU-RAMS and the use of analytical models for the Pasific 93 experiment, Vancouver, Canada. Good agreement between of the modelled and measured height of the IBL was obtained despite its complex structure in space and time [11].

Batchvarova and Gryning [12] describe the development of an IBL in the Athens area at the time of the international experiment MEDCAPHOT-TRACE 1994 to study the processes of distribution, photochemical transformation and transmission of pollutants with the ultimate goal of forming a strategy for better ambient air quality for the 2004 Olympic Games. Through a numerous of surface observations and vertical sounding systems with tethered balloons, IBL height of 400 m is found at 4 km from the coast and of 700 m at 13 km from the coast.

De Leo et al. [13] analyze sodar data and mesometeorological modeling of the breeze circulation in the area of Lamezia Terme, in the Tyrrhenian Sea in Calabria in the summer of 2007. The sodar data included in the work shows a clear alternation of positive vertical wind speeds during the day with airflow from the sea to the land (from the west) and negative at night from land to sea (east) airflow.

Prabha et al. [14] describe observations with sodar and the formation of a Thermal Internal Boundary Layer (TIBL) in sea breeze in India for 10 days in February 1998 under conditions of switching from winter to summer circulation. The sodar is located on land at a distance of 5 km from the shore, and the difference in land and water temperatures is from 0.5 to 3.5 K. In this situation, the measured TIBL height through the peak in the vertical dispersion profile is about 150–200 m. With higher temperature amplitude on the two main surfaces, the TIBL's height is expected to increase much faster with the sea breeze spread overland.

Petenko et al. [15] present a study of the turbulent characteristics and the height of the PBL at Concordia Station (Dome C) in Antarctica. The main measuring instrument is a sodar with an exceptional resolution of 2 m height and a range of about 200 m. This work discusses in detail the use of data as a source for the study of turbulence in PBL.

It can be noted that in the literature there is research dedicated to the coastal boundary layer using sodar measurements in many places around the world, but mainly for short periods or even days. These studies prove the great capabilities of acoustic remount sounding to study the wind and turbulent structure of the PBL, particularly in coastal areas. The analysis of long-term data proposed in this paper discloses the coastal nocturnal wind regime and turbulent structure in a region with modest observation networks in Bulgaria, but are of importance for coastal climatology in general. Except for theoretical research, the created database can be used for regime studies and evaluation of model performance in coastal areas.

2 Measuring Site and Equipment

Meteorological Observatory (MO) Ahtopol is located in the south-eastern part of the Bulgarian Black Sea coast (Fig. 1) at about 2 km southeast of the town of Ahtopol. The observatory falls into the Black Sea coastal Strandzha climate region, which is a part of the Black Sea climatic sub-region of Continental-Mediterranean climatic zone in Bulgaria [16]. Well expressed breeze circulation in the warm half of the year is typical for the climate in the region. Local circulation in the study area is observed throughout the year, whereas during the cold season a lower frequency and smaller time and spatial scales are registered [17].

MO Ahtopol is situated primarily on a flat grassland at about 400 m inland and 30 m height above sea level. The coast line is stretching out from NNW to SSE with a steep about 10 m high cost (Fig. 1). The observations are performed with an acoustic mono-static Doppler remote sensing system—SCINTEC Flat Array Sodar MFAS with a frequency range of 1650–2750 Hz, 9 emission/reception angles (0°, ±9.3°, ±15.6°, ±22.1°, ±29°), a vertical range from 150 to 1000 m and a vertical resolution of 10 m. The accuracy for wind speed is 0.1–0.3 ms^{-1} and for wind direction is 2–3° [18]. The sodar system is mounted on the roof of MO Ahtopol at about 4.5 m above

Fig. 1 Location of MO Ahtopol in southeastern Bulgaria on Google Earth (42° 5′ 3.37″ N, 27° 57′ 4.49″ E)

the ground. The data are recorded every 10 min and the average period is 20 min. The first measurement level is 30 m and the maximum vertical range for these study reaches 700 m.

3 Data and Analysis Overview

3.1 Data Availability

The exploration of coastal PBL characteristics in this work covers a 3014-day period from 1 August 2008 to 31 October 2016. The continuity of operation of the sodar was disturbed by frequent accidents of the main power supply and practically hampered remote technical support of the installed equipment by the lack of Internet access in observatory until 2011. In the summer months of 2008 and 2009, the sodar was stopped during the night hours. From 1st August to 31st October 2008 sodar measurements were made from 7:00 a.m. to 6:00 p.m. From 8th December 2008 to 27th July 2009 the sodar functioned continuously and after that until December 2009 only during the day, from 7:30 a.m. to 9:40 a.m. After December 2009 the sodar was worked continuously.

The data availability of the atmospheric acoustic sounding is presented in Table 1. The low data availability (yellow markings) during the summers of 2008 and 2009 is mainly due to the restrictions placed on the night mode of operation while in the other months it is due to the occurrence of interruption of electricity at MO Ahtopol.

Data with availability above 70% is given in green, between 40 and 70% in yellow, and below 40% in red. During the years of operating mode, the manufacturer provided periodic updates to the sodar software, resulting in a gradual increase in the optimal height of the output profiles while preserving the strict data quality control

Table 1 Monthly data availability and maximum effective height reached during the sodar operating mode for the period 01.08.2008–10.31.2016

	I	II	III	IV	V	VI	VII	VIII	IX	X	XI	XII
2008	-	-	-	-	-	-		45.2%	40.3%	57.7%	59.5%	88.4%
max range [m]	-	-	-	-	-	-		520	520	520	520	520
2009	99.9%	99.6%	99.2%	96.7%	98.3%	99.3%	94.6%	57.5%	59.9%	58.4%	96.7%	96.0%
max range [m]	520	520	680	680	680	680	680	680	680	680	680	680
2010	97.5%	98.3%	89.0%	68.5%	96.8%	86.4%	99.9%	98.3%	99.9%	92.6%	99.6%	99.8%
max range [m]	680	680	680	680	680	680	560	510	510	510	510	510
2011	96.8%	94.8%	99.8%	96.7%	96.8%	96.2%	92.2%	99.9%	38.8%	78.8%	99.2%	81.3%
max range [m]	510	460	510	510	510	510	510	510	560	620	620	620
2012	75.3%	95.8%	99.7%	96.7%	99.3%	93.3%	99.1%	31.9%	96.6%	30.6%	23.3%	100.0%
max range [m]	620	620	620	620	620	620	700	620	720	670	640	720
2013	96.6%	96.4%	50.6%	100.0%	98.3%	54.7%	95.3%	96.3%	96.7%	58.0%	74.7%	61.7%
max range [m]	720	720	720	620	680	670	680	680	720	720	720	720
2014	100.0%	99.9%	99.7%	100.0%	97.1%	99.8%	90.0%	59.4%	51.7%	98.5%	97.5%	98.0%
max range [m]	720	720	720	720	720	720	720	720	750	750	750	730
2015	99.9%	96.3%	94.9%	97.8%	69.5%	73.3%	57.4%	97.9%	99.5%	99.9%	65.9%	95.1%
max range [m]	750	750	750	750	750	750	590	750	750	750	750	730
2016	80.1%	70.0%	76.1%	49.9%	35.6%	93.2%	99.9%	93.0%	75.0%	45.4%	-	-
max range [m]	750	750	750	750	750	1000	1000	1000	1000	750	-	-

build into the sodar software and the spatial and temporal resolution of the data selected at the beginning of the atmospheric sounding at MO Ahtopol (July 2008). The maximum height specified in the measurement settings is not guaranteed. The actual height (effective) of the output profiles is determined by the availability of turbulent temperature inhomogeneous in the atmosphere above the sodar, which can return the signals to the antenna receiver. The actual sodar range is also presented graphically in Table 1 with one bar filled at a height of 510 m, 2 bars over 610 m, 3 bars over 710 m and 4 bars over 810 m. In this paper all profiles are studied up to 700 m due to low availability of data above that height.

3.2 Analysis

In this climatological study of coastal PBL vertical structure with high spatial and temporal resolution the direction from 0 to 120° is determined for marine air masses, while for the air masses from the land the direction is in the range between 170 and 290°. The entire 3014-day study period contains total of 2708 days with measurements, representing nearly 90% availability from all days from the total period. A summary of the analysis of the nocturnal marine air masses and those from the land is presented in Table 2. Conducted analyses of all land (brown color in Table 2) and marine (blue color in Table 2) air masses are deepened with study by season (cold and warm part of the years) for exploring seasonal variability of coastal PBL characteristics. The cold part of the years is defined from November to March and the warm period from May to September (Table 2—first column). Due to the presence of breeze circulation in the studied area, the number of profiles involved in the averaged characteristics of land air masses (10.5% from the total period) are significantly higher than marine air masses profiles (2.5% from the total period). The conditions for filtering the data for various analyses (fourth column at Table 2) are as follows:

Table 2 Types of long-term analyses of night coastal air masses by wind direction and different conditions

Period of analysis from 08/2008 to 10/2016 (total - 3014 days). Days with observations - 2708 days			
Analysis of land air masses /170 ÷ 290 Deg/	Height [m]	Available profiles	Conditions
Nocturnal air masses /21 ÷ 05h/ (45 549 profiles) 10.5 % from the total period	700/ 630/ 550*/ 450*/ 350*/ 320*/ 300*/ 270*/ 250*/ 150*	45 549/ 8 671/ 39*/ 244*/ 1 388*/ 2 027*/ 2 571*/ 3 523*/ 4 278* / 8022*	3/ 2/ 1*/ 1*/ 1*/ 1*/ 1*/ 1*/ 1*/ 1*/ 1*
Nocturnal /November÷ March/ (18 616 profiles) 4.3 % from the total period	700/ 630/ 550*/ 450*/ 350*/ 320*/ 300*/ 270*/ 250*/ 150*	18 616/ 4 458/ 21*/ 178*/ 799*/ 1 224*/ 1 596*/ 2 143*/ 2540* / 4262*	3/ 2/ 1*/ 1*/ 1*/ 1*/ 1*/ 1*/ 1*/ 1*/ 1*
Nocturnal /May ÷ September/ (18 769 profiles) 4.3 % from the total period	730/ 610/ 550*/ 450*/ 350*/ 320*/ 300*/ 270*/ 250*/ 150*	18 769/ 2 603/ 18*/ 37*/ 379*/ 504*/ 602*/ 811*/ 1 021* / 2 311*	3/ 2/ 1*/ 1*/ 1*/ 1*/ 1*/ 1*/ 1*/ 1*/ 1*
Analysis of marine air masses /0 ÷ 120 Deg/	Height [m]	Available profiles	Conditions
Nocturnal air masses /21 ÷ 05h/ (10 919 profiles) 2.5 % from the total period	700/ 590/ 550*/ 450*/ 350*/ 320*/ 300*/ 270*/ 250*/ 150*	10 919/ 3 731/ 3*/ 9* 25*/ 55*/ 89*/ 196*/ 400*/ 3 120*	3/ 2/ 1*/ 1* 1*/ 1*/ 1* 1*/ 1*/ 1*
Nocturnal /November÷ March/ (3 937 profiles) 0.9 % from the total period	700/ 340/ 320*/ 300*/ 270*/ 250*/ 150*	3 939/ 1 141/ 22*/ 36*/ 91*/ 159* / 854*	3/ 2/ 1*/ 1*/ 1* 1*/ 1*/ 1*
Nocturnal /May ÷ September/ (4 666 profiles) 1.1 % from the total period	700/ 590/ 550*/ 450*/ 350*/ 320*/ 300*/ 270*/ 250*/ 150*	4 666/ 1 863/ 3*/ 9* 21*/ 26*/ 35*/ 54*/ 151* / 1 654*	3/ 2/ 1*/ 1* 1*/ 1*/ 1* 1*/ 1*/ 1*

- 1*—continuous profiles to fixed heights with simultaneous availability of 12 sodar output parameters (wind direction/*WD*/, wind speed and its dispersion/*WS*, *sigWS*/, vertical wind speed and its dispersion/*W*, *sigW*/, horizontal wind speed components and their dispersions /*U*, *sigU*, *V*, *sigV*/, eddy dissipation rate /*EDR*/, turbulent intensity /*TI*/ and turbulent kinetic energy /*TKE*/);
- 2—continuous profiles with a minimum height of 110 m and simultaneous availability of 12 sodar output parameters;
- 3—profiles consisting of a minimum of 3 points in height satisfying the wind direction condition and permitting an interruption only for lack of data.

The complexity of different fulfilled conditions in the extracted profiles (1*, 2 or 3) determine the number of profiles involved in the various analyses (Table 2—third column) and the maximum height to which the average profiles reach (Table 2—second column). The lowest availability of profiles involved in averaging of coastal PBL characteristics is under condition 1*, due to its strength as filter—continuous profiles of 12 different simultaneous available parameters to fixed heights (150, 250, 270, 300, 320, 350, 450 and 550 m). The complexity of fulfilling this condition lies in the fact that measurements with remote sensing instruments may fail at some levels and lead to missing data at given altitudes or the algorithms for signal quality of the instrument may reject data at some levels.

As there is a need for aerosols in the atmosphere for the doppler lidars for uninterrupted data availability in profiles, there is a need for temperature inhomogeneities for the sodar. Thus, in areas with very low aerosol content, the lidars work is hampered. Similarly, the sodar work is hampered in areas with homogeneous temperature conditions. These features lead to different data availability in the averaged profiles at different heights and so impose the use of different analysis—all profiles with available data at least three points in height defined by condition 3 (though intermittently) or filtered data—samples that meet different conditions as 1* and 2. Using conditions 2 and 3 results in averaged profiles with not fixed-size and different data availability involved in calculating of certain mean value at a corresponding height while the condition 1* results in averaging of the same numbers of values across the entire height of the fixed-size averaged profile.

4 Averaged Vertical Profiles of Nocturnal Coastal Boundary Layer

Estimating the PBL height through the turbulent profiles characteristics (*sigW*, *TKE*, *BP*, etc.) has been suggested in recent years in studies based on data from remote sensing measurements [5, 19].

In the absence of temperature and humidity profiles in the atmosphere, such analyses make it possible to retrieve more information from wind data. While with the lidars the calculations of *sigW* are based on a backscatter signals from aerosols, the measurement of turbulent characteristics with the sodars is direct. In this paper, all profiles of the turbulent parameters are presented and explored first as information from all long-term measurements with given characteristics and then divided by cold and warm part of the year. The nocturnal PBL falls better in the range of the sodar which allows to assess its characteristics, including its height.

4.1 Nocturnal Land Air Masses

All nocturnal land air masses and condition 3

Characteristics of all nocturnal land air masses are shown in Fig. 2 (averaged 45,549 individual profiles representing 10.5% of the total period—Table 2) through 12 averaged profiles (red lines with color dots) and their dispersions (green area). The color dots have indicated the availability of the individual profiles involved in the averaging at given altitudes. The lowest profiles availability was observed in 4 parameters (*sigWS*, *sigU*, *sigV* and *TI*) due to the fact that they are calculated from the sodar software as a second statistical moment of the corresponding sodar parameters, requiring higher quality control of the individual measurements compared to the first statistical moments, such as the wind components. An approximate linear increase in the wind

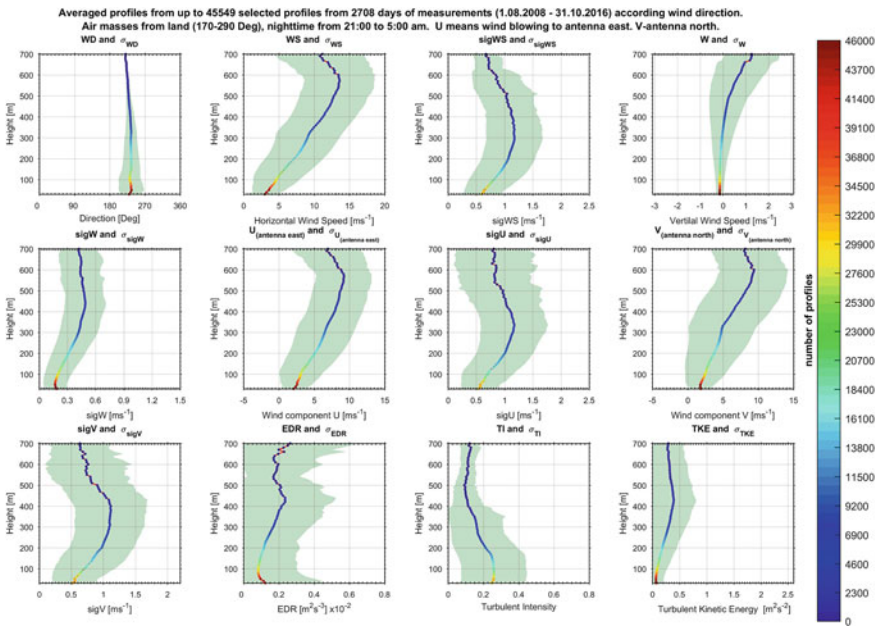

Fig. 2 Averaged nocturnal land air masses characteristics with condition 3. Mean profiles and their dispersions from left to right and from top to bottom: *WD*, *WS*, *sigWS*, *W*, *sigW*, *U*, *sigU*, *V*, *sigV*, *EDR*, *TI*, *TKE*

speed profile is observed up to a height of 540 m above the surface (1318 individual profiles available at that height) resulting in a more than quadruple value compared to the lowest point of the averaged profile (30 m above the surface). Positive values after 340 m are seen in the vertical wind speed profile (12,227 individual profiles) and increase faster above 500 m. Slightly expressed peaks in the shape of the *sigW*, *EDR* and *TKE* profiles are observed at 430 m with respectively 3625, 1756 and 3011 individual profiles involved in the averaged outputs at this altitude. The surface layer (SL) height is defined between 50 and 100 m with *sigW*, *EDR* and *TKE* characteristics change.

Nocturnal land air masses and condition 2 during the warm part of the year

Averaged nocturnal land air masses during the period from May to September are presented in Fig. 3. The individual profiles used for the calculations of the mean values are close to 30% of all registered nocturnal land air masses with the same performed condition 2 (Table 2). Well expressed changes in the shape of averaged profiles after 400 m are observed at almost all graphs. The peaks in the sigW, EDR and TKE mean profiles are at the same height of 410 m above the ground (98 individual profiles involved at this height). Almost a linear decrease in the averaged TI profile is observed after the main peak at 140 m (2412 individual profiles) and it is interrupted by a second smaller peak at 430 m (59 individual profiles). This type of profiles,

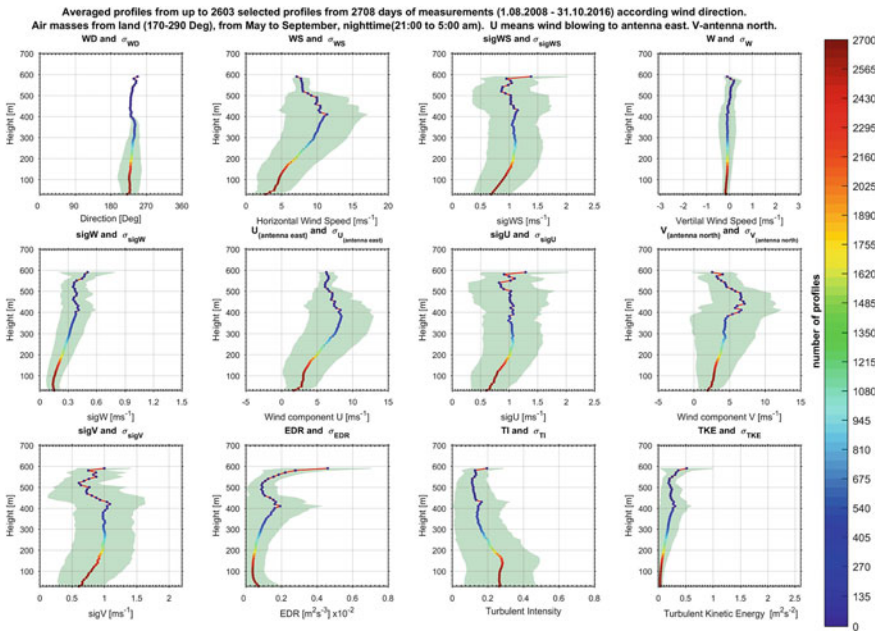

Fig. 3 Averaged nocturnal land air masses characteristics during warm part of the year with imposed condition 2. Details as in Fig. 2

characterizing nocturnal land air masses during the warmer part of the year, is the reason for the less pronounced peak observed in the mean sigW, EDR and TKE profiles in Fig. 2 at an altitude of 430 m. Close to the ground at a height between 50 and 80 m the SL height is defined with changes in sigW, EDR, TI and TKE profiles.

4.2 Nocturnal Marine Air Masses

Nocturnal marine air masses during the cold part of the year and condition 3

The mean values of up to 3937 individual profiles are used for the averaged profiles and their dispersions output at the 12 graphs in Fig. 4. The characteristics of nocturnal marine air masses meeting conditions 3 from November to March are presented. Noticeable peaks are seen at the averaged *sigW* and *TKE* profiles (respectively 406 and 289 individual profiles) with a change in the character of the profiles at a height of 300 m above the ground. Such a pronounced peak is also observed with the average *EDR* profile, but at height of 340 m (103 individual profiles). The nocturnal marine air masses during the cold part of the year are defined by the winter profiles and partly by these in the transition seasons at which the synoptic conditions with eastern and northeastern wind components were dominant. Therefore, in this case, we associate

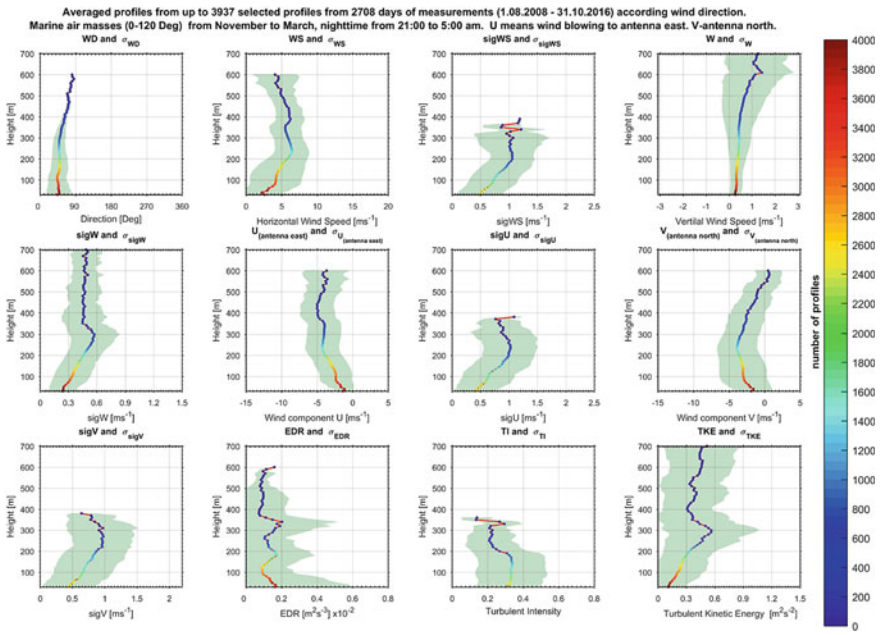

Fig. 4 Averaged nocturnal marine air masses characteristics during cold part of the year with performed condition 3. Details as in Fig. 2

the observed *sigW* and *TKE* peaks at a height of 300 m, with a slightly unstable or neutral marine PBL height, due to the relatively warm sea surface during the cold part of the year. A weakly pronounced positive peak at 40–50 m from the ground at *TI* profile, supported by the almost constant values of *sigW* up to 50 m and *EDR* up to 40 m, as well as the observed weak peaks of *WD*, *WS* and *W* at 40 m can be associated with height of the IBL formed by a dominant factor the surface roughness change.

Using the dispersion of the vertical wind speed *sigW* (σ_w) measured from the sodar at different altitudes (z), the Buoyancy Production (*BP*) profiles can be derived from (1):

$$\beta = \frac{{\sigma_w}^3}{z} \tag{1}$$

Averaged *BP* profiles characterizing the nocturnal marine air masses during the cold part of the year with performed condition 1* and 3 (left and right graphic respectively) are derived from Eq. (1) and are presented in Fig. 5, confirming the comments made so far about observed peaks and altitudes in the averaged profiles and their dispersions (Fig. 4). The flow of Archimedes force (buoyancy flow) or the assessment of turbulence generation due to convection is expected and has high values near the ground and decreases with height to reach the value distinctive for

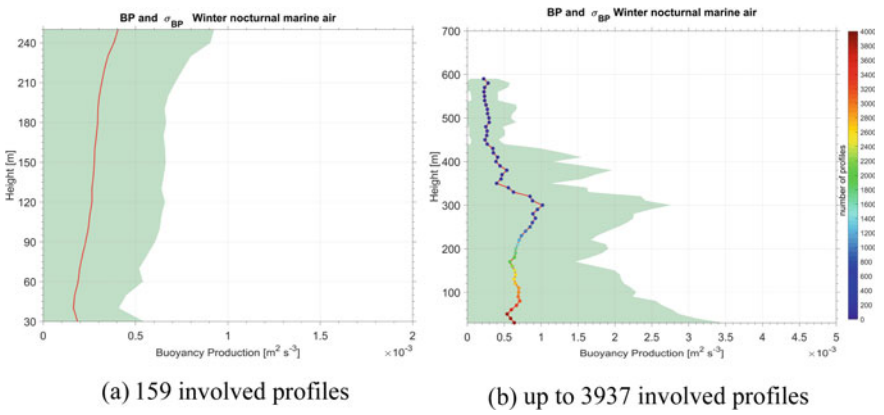

Fig. 5 Averaged buoyancy production profiles from nocturnal marine air masses with performed conditions 1* (**a**) and condition 3 (**b**) from November to March

the higher layer in the atmosphere. High *BP* values can also be expected in the interaction or entrainment zone over a convective boundary layer where transport of warmer air masses from the stable layer aloft takes place. The averaged nocturnal *BP* profile that is calculated from 159 individual profiles at which the condition 1* was fulfilled (Fig. 5a) decreases its values to 40 m, and thus with Condition 3 (Fig. 5b) to 50 m. These negative peaks are an indicator of convective or neutral IBL and non-disturbed marine air masses over it during the night. Under condition 3 (Fig. 5b) there is a pronounced peak at 300 m above ground, thus confirming that at night in the cold season the height of the marine PBL (slightly unstable or neutral) is about 300 m.

4.3 Thermodynamic State of Nocturnal Air Masses

The seasonal diagrams of stability classes probabilities at different heights are shown in Fig. 6. The atmospheric stability classes according to the Pasquill–Gifford classification using the σ_ϕ method [20] are defined by two main types of nocturnal individual profiles with applied condition 2. The sum of all probabilities at a given altitude is considered as 100% based on all available time series with disposable data for the respective altitude.

According to the classification used, the probabilities range mainly from 38 to 78% with mean value of 59% for the slightly stable stratification (E) of the nocturnal land air masses during the warm part of the year (Fig. 6a). Neutral stratification (D) can be indicated as the second dominant thermodynamical state of the atmosphere for this type of air masses with probability distribution values in the rage mainly from 17 to 29% and maximum of about 62% at 570 m and 22% mean value. The dominant class of atmospheric stratification for nocturnal land air masses during

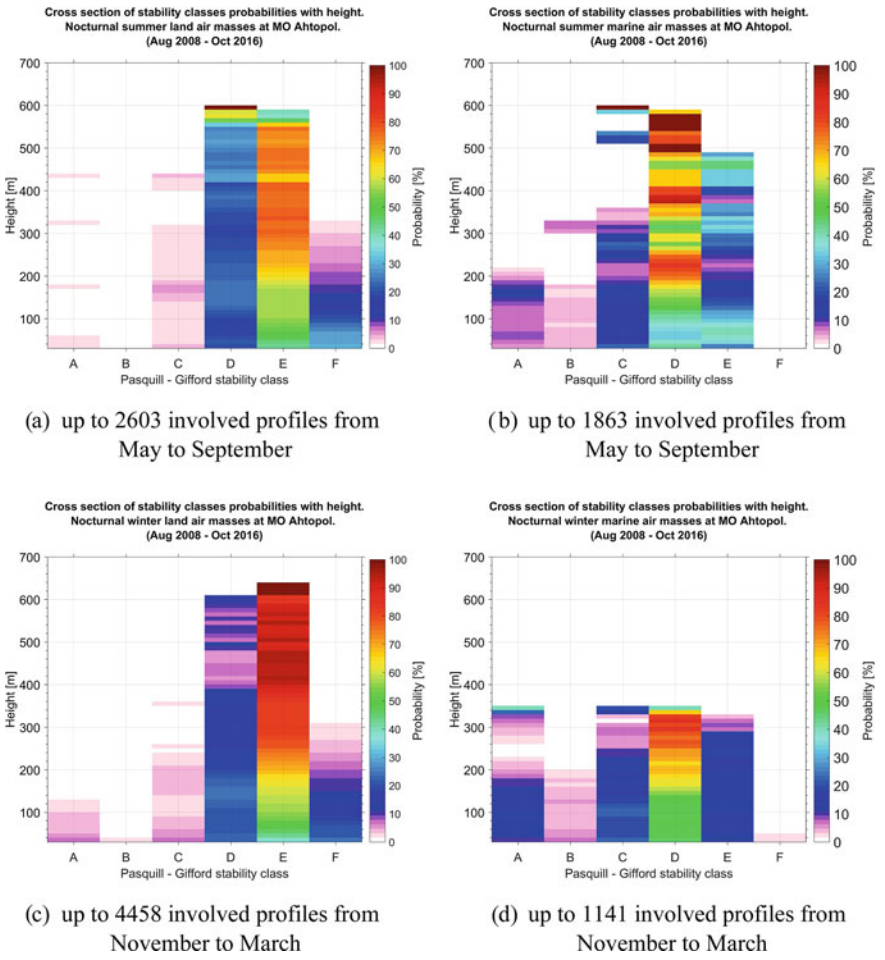

Fig. 6 Diagrams of stability classes probabilities at different heights (warm season—**a**, **b**; cold season—**c**, **d**) of nocturnal land (**a**, **c**) and marine (**b**, **d**) air masses with performed condition 2

the cold part of the year (Fig. 6c) can be indicated as the slightly stable (E) with more than 50% probability after 70 m and more than 70% after 200 m *AGL* with 63% mean value throughout the acoustic sounding layer. In this type of air masses, the results of stability classes probabilities with height have determined the neutral stratification again as the second dominant class with an average value of 20%. The stable stratification (F) is presented in both types of nocturnal land air masses as the third dominant class of atmospheric stratification with mean probability about 16% for the warm period and 11% for the cold one. The mean probability values of extremely unstable (A) classes have been respectively about 2 and 3% while for moderately unstable classes (B) have been below 0.7 and 0.5%.

The changes in the stratification of nocturnal marine air masses during the warm and cold part of the year are shown on the right side of Fig. 6. Compared to the graphs of land profiles, the marine air masses have revealed more unstable thermodynamical state of the atmosphere. Neutrally stratified atmosphere (D) is observed as dominant stratification in nocturnal marine air masses with minimum probability values of 33% and mean 49% for the warm part of the year and minimum 46% and mean 54% for the cold pat of the year. The largest instability and the variations of thermodynamical state of all cases considered in Fig. 6 are observed in the averaged profiles of nocturnal marine air masses during the cold season (Fig. 6d).

5 Conclusions

The presented results for all nocturnal land air masses with applied condition 3 show a super position of all seasonal profiles with imposed minimum restriction in their selection. Reducing the number of selected profiles only during the warm part of the year with applied condition 2, the achieved results are confirmed.

The analysis is based on 82% of the data on nocturnal land air masses. The nocturnal air masses from the land are characterized by prevailing conditions between neutral and slightly stable stratification. Indications of a nocturnal stable PBL height at 410–430 m and corresponding SL height of 50–80 m are found.

Prevailing conditions of neutral and slightly unstable stratification are revealed in the results for nocturnal marine air masses. Indications of nocturnal IBL height of about 40–50 m and a nocturnal marine PBL height of about 300 m are found.

This study is based on reliable long term acoustic remote sensing data and it is of great importance for diagnostic or prognostic air pollution modelling and could support related adequate decision-making actions of governments and business for better air quality, citizens health protection and tourism development in a coastal zone. Such analyses allow not only climatological studies for a number of PBL parameters, but also to assess the fraction of time when theoretical profiles can be used in coastal areas. The performance of weather and climate models in coastal areas can be improved if assessed with such types of long-term wind and turbulence vertical profiles data.

Acknowledgements This work was partially supported by the Bulgarian Ministry of Education and Science under the National Research Programme "Young scientists and postdoctoral students" approved by DCM #577/17.08.2018 and by the National Science Fund of Bulgaria, Contract KP-06-N34/1 "Natural and anthropogenic factors of climate change—analyses of global and local periodical components and long-term forecasts".

References

1. Cimini, D., Marzano, F.S., Visconti, G.: Integrated Ground-Based Observing Systems. Springer-Verlag, Berlin Heidelberg (2011)
2. Coulter, R.L., Kallistratova, M.A.: Two decades of progress in SODAR techniques: a review of 11 ISARS proceedings. Meteorol. Atmos. Phys. **85**, 3–19 (2004). https://doi.org/10.1007/s00703-003-0030-2
3. Engelbart, D., Monna, W., Nash, J., Mätzler, C.: Integrated ground-based remote-sensing stations for atmospheric profiling: COST action 720: final report. In: Engelbart, D., Monna, W., Nash, J., Mätzler, C. (eds.) p. 398. Publications Office of the European Union—COST Office, Luxembourg (2009)
4. Emeis, S.: Surface-based remote sensing of the atmospheric boundary layer, vol. 40, 1st edn. Atmospheric and Oceanographic Sciences Library. Springer Netherlands (2011)
5. Illingworth, A., Ruffieux, D., Cimini, D., Lohnert, U., Haeffelin, M., Lehmann, V.: COST Action ES0702 Final Report: European Ground-Based Observations of Essential Variables for Climate and Operational Meteorology. In: COST Action ES0702 EG-CLIMET, p. 141. COST Office, PUB1062 (2013)
6. Peña, A., Floors, R.R., Sathe, A., Gryning, S.-E., Wagner, R., Courtney, M., Larsén, X.G., Hahmann, A.N., Hasager, C.B.: Ten years of boundary-layer and wind-power meteorology at Høvsøre, Denmark. Boundary-Layer Meteorol. **158**(1), 1–26 (2016). https://doi.org/10.1007/s10546-015-0079-8
7. Batchvarova, E.: Theoretical and Experimental Studies of the Atmospheric Boundary Layerover Different Surface Types. National Institute of Meteorology and Hydrology (NIMH) and the Bulgarian Academy of Sciences (BAS) (2006)
8. Hsu, S.A.: A note on estimating the height of the convective internal boundary layer near shore. Bound.-Layer Meteorol. **35**(4), 311–316 (1986). https://doi.org/10.1007/BF00118561
9. Simpson, J.E.: Sea Breeze and Local Winds. Cambridge University Press, Cambridge, UK (1994)
10. Wilczak, J.M., Dabberdt, W.F., Kropfli, R.A.: Observations and numerical model simulations of the atmospheric boundary layer in the Santa Barbara coastal region. J. Appl. Meteorol. **30**(5), 652–673 (1991). https://doi.org/10.1175/1520-0450(1991)030%3c0652:OANMSO%3e2.0.CO;2
11. Batchvarova, E., Cai, X., Gryning, S.-E., Steyn, D.: Modelling internal boundary-layer development in a region with a complex coastline. Bound.-Layer Meteorol. **90**(1), 1–20 (1999). https://doi.org/10.1023/A:1001751219627
12. Batchvarova, E., Gryning, S.-E.: Wind climatology, atmospheric turbulence and internal boundary-layer development in Athens during the MEDCAPHOT-TRACE experiment. Atmos. Environ. **32**(12), 2055–2069 (1998). https://doi.org/10.1016/S1352-2310(97)00422-6
13. De Leo, L., Federico, S., Sempreviva, A.M., Pasqualoni, L., Avolio, E., Bellecci, C.: Study of the development of the sea breeze and its micro-scale structure at a coastal site using a multi-tone sodar system. In: 14th International Symposium for the Advancement of Boundary Layer Remote Sensing, 23–25 June 2008, Copenhagen, Denmark 2008. IOP Conference Series: Earth and Environmental Science, p. 9. 2008 IOP Publishing Ltd.
14. Prabha, T.V., Venkatesan, R., Mursch-Radlgruber, E., Rengarajan, G., Jayanthi, N.: Thermal internal boundary layer characteristics at a tropical coastal site as observed by a mini-SODAR under varying synoptic conditions. J. Earth Syst. Sci. **111**(1), 63–77 (2002). https://doi.org/10.1007/BF02702223
15. Petenko, I., Argentini, S., Casasanta, G., Kallistratova, M., Sozzi, R., Viola, A.: Wavelike structures in the turbulent layer during the morning development of convection at Dome C, Antarctica. Bound.-Layer Meteorol. 1–19 (2016). https://doi.org/10.1007/s10546-016-0173-6
16. Sabev, L., Stanev, S.: Climate Regions of Bulgaria and Their Climate, vol. V. State Publishing House "Science and Art", Sofia, Bulgaria (1959)

17. Barantiev, D., Batchvarova, E., Novitsky, M.: Breeze circulation classification in the coastal zone of the town of Ahtopol based on data from ground based acoustic sounding and ultrasonic anemometer. Bulgarian J. Meteorol. Hydrol. (BJMH) **22**(5) (2017)
18. ScintecAG: Scintec Flat Array Sodars—Hardware Manual (SFAS, MFAS, XFAS) including RASS RAE1 and windRASS, Version 1.03 ed. Scintec AG, Germany (2011)
19. Illingworth, A.J., Cimini, D., Gaffard, C., Haeffelin, M., Lehmann, V., Löhnert, U., O'Connor, E.J., Ruffieux, D.: Exploiting existing ground-based remote sensing networks to improve high-resolution weather forecasts. Bull. Am. Meteor. Soc. **96**(12), 2107–2125 (2015). https://doi.org/10.1175/BAMS-D-13-00283.1
20. Bailey, D.T.: Meteorological monitoring guidance for regulatory modeling applications. In: Standards, O.O.A.Q.P.A. (ed.) p. 171. United States Environmental Protection Agency (EPA), Research Triangle Park, NC 27711 (2000)